PHYSICAL REVIEW D **90,** 074004 (2014)

Influence of threshold effects induced by charmed meson rescattering

Xiao-Hai Liu[*]

Department of Physics and State Key Laboratory of Nuclear Physics and Technology, Peking University, Beijing 100871, China

(Received 16 March 2014; published 2 October 2014)

We investigate the processes e^+e^- annihilating to $J/\psi\pi\pi$, $\psi'\pi\pi$ and $h_c\pi\pi$. The coupled-channel effects induced by the couplings between the widely accepted D-wave charmonium $\psi(4160)$ and D_1D, D_1D^* and D_2D^* charmed meson pairs in the S-wave state with couplings given by heavy quark spin symmetry are analyzed. The line shapes show the presence of cusps that result from the singularities of the rescattering loops, which could be helpful in understanding the nature of $Y(4260)$, $Y(4360)$, $Z_c(3900)/Z_c(3885)$ and $Z_c(4020)/Z_c(4025)$.

DOI: 10.1103/PhysRevD.90.074004 PACS numbers: 13.25.Gv, 13.75.Lb, 14.40.Pq

I. INTRODUCTION

There has been a renewal of QCD spectroscopy in the past decade, initiated by the findings of numerous XYZ states near the open-flavor thresholds. Most of these states do not fit into the predictions of the quenched potential quark model, which has been proved to be very successful in describing the conventional heavy quarkonia below the open-flavor threshold. These inconsistences remind people that the vacuum polarization effect of dynamical fermions should receive more attention in understanding the heavy quarkonium spectroscopy. This vacuum polarization effect could be described by the coupled-channel effects induced by the couplings between heavy quarkonia and open-flavor mesons. After taking into account the coupled-channel effects, the masses and decay properties of the heavy quarkonia will be changed significantly, especially when the masses of the heavy quarkonia are close to the corresponding open-flavor thresholds [1–9].

The mysterious charmonium-like state $Y(4260)$ has many peculiar properties. As a charmonium candidate, it is observed in the $J/\psi\pi\pi$ channel, but not in the open-charm decay channels which are supposed to be favorable decay modes of conventional $c\bar{c}$ states. The R-value scan around 4.26 GeV also appears to have a dip instead of a bump structure. The state observed in the $\psi'\pi\pi$ channel, $Y(4360)$, has similar puzzles as those of $Y(4260)$. Recent experimental observations revive discussions on the nature of $Y(4260)$. Several charged charmonium-like structures, $Z_c(3900)$, $Z_c(3885)$, $Z_c(4020)$ and $Z_c(4025)$, are observed while studying $Y(4260)$ [10–15], which makes $Y(4260)$ more intriguing. We refer to Refs. [16,17] for a recent review about these XYZ states.

Since the masses of excited charmed mesons are usually larger, the influence of coupled-channel effects on charmonia with the P-wave charmed mesons (D_0, D_1, etc.) involved has not been widely studied before. On the other hand, the thresholds of the combinations of S- and P-wave charmed mesons are very close to $Y(4260)$ and $Y(4360)$, and their couplings with the parity-odd charmonia could be S wave, which is supposed to be strong. In this paper, we will study the influence of the coupled-channel effects on the line shapes of some pertinent cross sections and invariant mass distributions, where the contributions with P-wave charmed mesons involved are emphasized.

II. COUPLED-CHANNEL EFFECTS IN THE DIPION TRANSITIONS

We will build our model within the framework of heavy hadron chiral perturbation theory (HHChPT). In HHChPT, to encode the heavy quark spin symmetry (HQSS), the doublets with light degrees of freedom (LDOF) $J^P = 1/2^-$, $1/2^+$, $3/2^+$ are collected into three superfields:

$$H_a = \frac{1+\not{v}}{2}[\mathcal{D}^*_{a\mu}\gamma^\mu - \mathcal{D}_a\gamma_5], \tag{1}$$

$$S_a = \frac{1+\not{v}}{2}[\mathcal{D}'^\mu_{1a}\gamma_\mu\gamma_5 - \mathcal{D}^*_{0a}], \tag{2}$$

$$T^\mu_a = \frac{1+\not{v}}{2}\left\{\mathcal{D}^{\mu\nu}_{2a}\gamma_\nu - \sqrt{\frac{3}{2}}\mathcal{D}_{1a\nu}\gamma_5\left[g^{\mu\nu} - \frac{1}{3}\gamma^\nu(\gamma^\mu - v^\mu)\right]\right\}, \tag{3}$$

respectively, where a is the light flavor index. For clarity, in the following, we will use HH to represent $D^{(*)}D^{(*)}$ combinations, with the similar conventions for TH and SH. The S-wave charmonia $\psi(nS)$ may couple to HH and SH via relative P and S wave respectively, where n denotes the radial quantum number. Required by HQSS, the total angular momentum of LDOF should also be conserved for these couplings. For the TH combination, their LDOF carry angular momentum $3/2$ and $1/2$ respectively. In an S-wave coupling, they cannot produce zero angular momentum carried by LDOF of $\psi(nS)$. As a result, the

[*]liuxiaohai@pku.edu.cn

S-wave coupling between $\psi(nS)$ and TH, although allowed by the parity conservation, will be suppressed according to HQSS [18]. In the heavy quark limit, the only allowed coupling is D wave. However, for the coupling between D-wave charmonia $\psi(nD)$ and TH, the S-wave coupling is allowed, since the total angular momentum of the LDOF of $\psi(nD)$ is 2. This gives us a hint that the coupled-channel interactions between $\psi(nD)$ and TH may largely affect the mass and decay properties of $\psi(nD)$, especially for the D-wave charmonia close to TH thresholds. In the charmonium family, $\psi(4160)$ is widely considered as a conventional 2^3D_1 charmonium, whose mass and width are estimated by PDG to be $M_\psi = 4153 \pm 3$ MeV and $\Gamma_\psi = 103 \pm 8$ MeV [19]. If we use the latest data, its mass and width are found to be $M_\psi = 4191.7 \pm 6.5$ MeV and $\Gamma_\psi = 71.8 \pm 12.3$ MeV in Ref. [20], or $M_\psi = 4193 \pm 7$ MeV and $\Gamma_\psi = 79 \pm 14$ MeV in Ref. [21], which are very close to TH thresholds and the mass of $Y(4260)$. Therefore it is natural to wonder whether there is some kind of connection between these states and the TH coupled channels. For further discussion, we mention that HH may couple to $\psi(nD)$ via the P wave, and the S-wave coupling between SH and $\psi(nD)$ is also suppressed according to HQSS. SH may couple to $\psi(nS)$ via the S wave. We show the HQSS allowed couplings in Table I to make the above points clear.

There are plenty of data for e^+e^- annihilating to one heavy quarkonium plus two pion mesons. Many interesting phenomena have been discovered in these channels. We will investigate these exclusive processes in this paper to try to quantify the coupled-channel effects. Taking into account the previous discussions, using HHChPT power counting we introduce the leading order effective Lagrangian as follows:

$$\begin{aligned}\mathcal{L}_1 = & \frac{g_T}{\sqrt{2}}\langle J^{\mu\nu}\bar{H}_a^\dagger\gamma_\nu\bar{T}_{a\mu} - J^{\mu\nu}\bar{T}_{a\mu}^\dagger\gamma_\nu\bar{H}_a\rangle \\ & + ig_H\langle J^{\mu\nu}\bar{H}_a^\dagger\gamma_\mu\overleftrightarrow{\partial}_\nu\bar{H}_a\rangle + g_S\langle J\bar{S}_a^\dagger\bar{H}_a + J\bar{H}_a^\dagger\bar{S}_a\rangle \\ & + C_S\langle J\bar{H}_b^\dagger\gamma_\mu\gamma_5\bar{H}_a\mathcal{A}_{ba}^\mu\rangle + iC_P\langle J^\mu\bar{H}_b^\dagger\sigma_{\mu\nu}\gamma_5\bar{H}_a\mathcal{A}_{ba}^\nu\rangle \\ & + \text{H.c.}, \end{aligned} \tag{4}$$

where $\langle\cdots\rangle$ means the trace over Dirac matrices, $\mathcal{A}^\mu$ is the chiral axial vector containing the Goldstone bosons, and the fields for the S-, P-, and D-wave charmonia read

$$\begin{aligned} J &= \frac{1+\not{v}}{2}[\psi(nS)^\mu\gamma_\mu]\frac{1-\not{v}}{2}, \\ J^\mu &= \frac{1+\not{v}}{2}[h_c(nP)^\mu\gamma_5]\frac{1-\not{v}}{2}, \\ J^{\mu\nu} &= \frac{1+\not{v}}{2}\left\{\psi(nD)_\alpha\left[\frac{1}{2}\sqrt{\frac{3}{5}}[(\gamma^\mu - v^\mu)g^{\alpha\nu} + (\gamma^\nu - v^\nu)g^{\alpha\mu}]\right.\right. \\ &\quad \left.\left. - \sqrt{\frac{1}{15}}(g^{\mu\nu} - v^\mu v^\nu)\gamma^\alpha\right]\right\}\frac{1-\not{v}}{2}, \end{aligned} \tag{5}$$

TABLE I. HQSS allowed couplings.

	HH	SH	TH
$\psi(nS)$	P wave	S wave	D wave
$\psi(nD)$	P wave	D wave	S, D wave

respectively, where only the states relevant for our discussion are included. The effective Lagrangian for the strong interactions of heavy mesons with Goldstone bosons reads

$$\begin{aligned}\mathcal{L}_2 = & i\frac{h'}{\Lambda_\chi}\langle\bar{H}_aT_b^\mu\gamma^\nu\gamma_5(D_\mu\mathcal{A}_\nu + D_\nu\mathcal{A}_\mu)_{ba}\rangle \\ & + ih\langle\bar{H}_aS_b\gamma_\mu\gamma_5\mathcal{A}_{ba}^\mu\rangle + ig\langle H_b\gamma_\mu\gamma_5\mathcal{A}_{ba}^\mu\bar{H}_a\rangle. \end{aligned} \tag{6}$$

Some of these Lagrangians have been introduced in Refs. [22–27], we refer to Ref. [23] for a review and some conventions.

The coefficient g_T in Eq. (4), which describes the coupling strength between $\psi(nD)$ and TH, is not well determined. But taking into account the coupling is S wave, it may be expected to be large. There are some indirect experimental evidences to support this argument. For instance, $\psi(4415)$ is a widely accepted S-wave charmonium, its decaying to D_2D is a D-wave decay, but the branching fraction is very large, which is $(10 \pm 4)\%$ estimated by PDG [19]. Therefore it seems to be reasonable to expect the S-wave coupling constant g_T could also be sizable. Of course this is not a serious estimation, to obtain some less model-dependent result, we will only focus on the line shape behavior of the total and differential cross sections of the pertinent channels in this paper.

The Feynman diagrams which contribute to the dipion transitions are displayed in Fig. 1, where we will take $\psi(4160)$ as the most relevant $\psi(nD)$ state, and use its PDG averaged mass and width as the input parameters in our calculation. Although the production of D-wave charmonia in e^+e^- annihilation is supposed to be suppressed, the experimental data indicates the electron decay width of $\psi(4160)$ is not small, i.e., $\Gamma_{ee} = (0.83 \pm 0.07)$ KeV [19], which possibly results from the S-D mixing effect. However, we still face a dilemma here. The larger electron decay width of $\psi(4160)$ implies the HQSS breaking effects, or some higher order contributions in the effective theory, may also be important, which can be ascribed to the fact that the charm quark is not so heavy. For the moment we will ignore some symmetry breaking effects, such as the breaking in the couplings between $\psi(nD)$ and TH, and still follow the guidance of HQSS (see Refs. [18,28] for some discussions on the symmetry breaking effects).

For the tree diagram displayed in Fig. 1(a), its amplitude will be proportional to a Breit-Wigner form function

$$BW[\psi(4160)] = (s - M_\psi^2 + iM_\psi\Gamma_\psi)^{-1}, \tag{7}$$

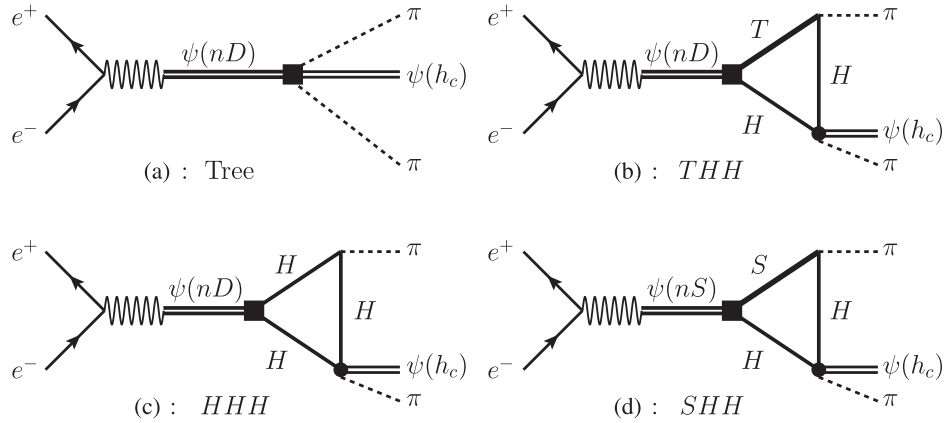

FIG. 1. Feynman diagrams for the dipion transitions.

where s is the center of mass energy squared. The cross section line shape of this diagram will be ordinary, which is just the usual Breit-Wigner structure, but it can provide some background that may affect the line shape behavior via interference.

For the triangle diagrams which describe the coupled-channel effects, there are several kinds of singularities corresponding to them. The location of the singularities in the complex space of the external momentum variables can be determined by a set of equations, which are usually called the Landau equations [29]. In some special kinematic configurations, all of the three internal lines can be on shell simultaneously, which corresponds to the *leading singularity* of the triangle diagram [30]. The singularities that correspond to two of the internal lines being on shell are *lower-order singularities* [30]. For the triangle diagram, the location of the *leading singularity* corresponds to the *anomalous threshold*, while the *lower-order singularity* corresponds to the *normal threshold* [30–32]. For instance, in Fig. 2, when $W = m_1 + m_3$, the *anomalous threshold* $\bar{s}_2$ in the complex s_2 plane is real, and

$$\bar{s}_2 = s_n + \frac{m_1}{m_3}[(m_2 - m_3)^2 - m^2], \tag{8}$$

where s_n is the *normal threshold* $(m_1 + m_2)^2$, and we have assumed the internal particles are stable. The above triangle singularities (TS) are usually branch points of the amplitude in the complex space. When the singularities approach close to the physical region, they may affect the threshold behavior of the physical amplitude dramatically, or show up

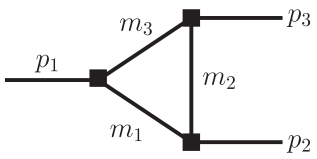

FIG. 2. Triangle diagram under discussion. For the external momenta, we define $p_1^2 = W^2$, $p_2^2 = s_2$, and $p_3^2 = m^2$.

directly as bumps or cusps in the amplitude [30,31,33–35]. The THH loops in our discussion just approximately meet the kinematic conditions of the leading TS, and for the charmed meson loops, according to Eq. (8), the *anomalous threshold* and *normal threshold* are very close to each other. We therefore expect these TS may lead to some detectable effects for the relevant processes.

Concerning Fig. 1(b), named as THH loop in this paper, there are four subdiagrams categorized by the intermediated charmed mesons:

(I) $\{D_1 D[D^*]\}$,
(II) $\{D_1 D^*[D^*]\}$,
(III) $\{D_2 D^*[D]\}$,
(IV) $\{D_2 D^*[D^*]\}$,

where the charmed mesons in the brackets correspond to the vertical propagators in the THH loops. For $J/\psi(\psi')\pi\pi$ final states, the amplitudes corresponding to the above four subdiagrams have a simple relation in the heavy quark limit, i.e.,

$$\mathcal{M}^I : \mathcal{M}^{II} : \mathcal{M}^{III} : \mathcal{M}^{IV} = 1 : \frac{1}{2} : -\frac{1}{5} : \frac{3}{10}. \tag{9}$$

This implies the main contribution may come from the $\{D_1 D[D^*]\}$ loop. For $\psi(nD) \to h_c\pi\pi$, the spin of the charm quark is flipped, which means this process is forbidden in the heavy quark limit. However, since we are using physical masses as input in the calculation and the masses of charmonia and charmed mesons are not so heavy, the amplitude still could be sizable. In Fig. 3, we display the line shapes of the energy dependence of the cross sections for $e^+e^- \to J/\psi\pi\pi$, $\psi'\pi\pi$ and $h_c\pi\pi$ via the D-wave state $\psi(4160)$ and THH loops. For the $J/\psi\pi\pi$ channel, apart from the $\psi(4160)$ bump, three cusps appeared at the thresholds of $D_1 D$, $D_1 D^*$ and $D_2 D^*$ respectively. Among these cusps, the one staying around the $D_1 D$ threshold is the most obvious one, which can be understood according to Eq. (9). The peak position of $\psi(4160)$ is upward shifted because of the interference with the $D_1 D$ cusp. For $\psi'\pi\pi$ and $h_c\pi\pi$ channels, the $\psi(4160)$ bump is

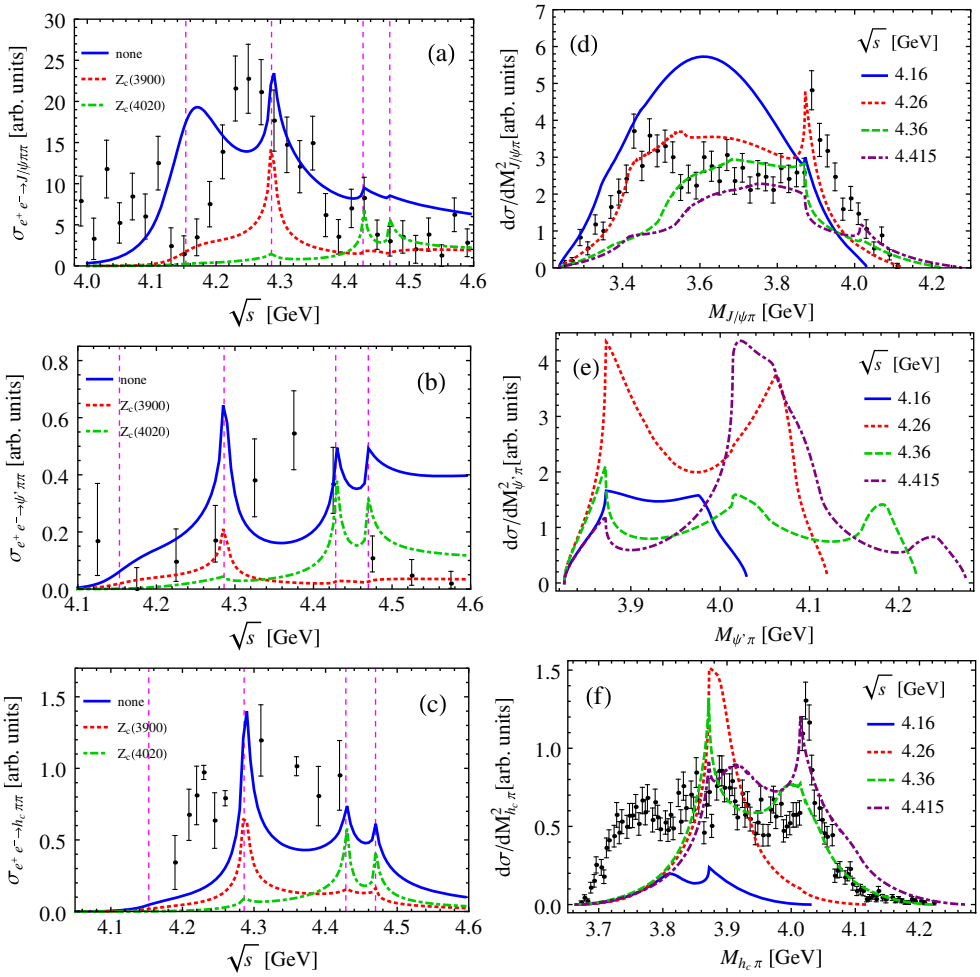

FIG. 3 (color online). Left: Energy dependence of the cross section for $e^+e^- \to$ (a) $J/\psi\pi\pi$, (b) $\psi'\pi\pi$, and (c) $h_c\pi\pi$ via $\psi(4160)$ and intermediate THH loops. The solid line is the result with only taking into account the contact interaction, the dotted and dot-dashed lines correspond to the result with plugging into $Z_c(3900)$ and $Z_c(4020)$ propagator respectively, and the magnitude of these lines has been rescaled to a similar level. The vertical lines (from left to right) indicate the mass of $\psi(4160)$, the thresholds of D_1D, D_1D^* and D_2D^* respectively. Right: The corresponding invariant mass distributions of (d) $J/\psi\pi$, (e) $\psi'\pi$, and (f) $h_c\pi$ at four center of mass energy points. Only the contact interactions are taken into account in THH loops. The experimental data are taken from Ref. [36] for (a), Ref. [37] for (b), Ref. [12] for (c), Ref. [10] for (d), and Ref. [12] for (f) respectively. The data points are rescaled to adapt the theoretical lines.

nearly smeared since the D_1D cusp is much stronger. This can be attributed to the thresholds of $\psi'\pi$ and $h_c\pi$ are much closer to that of HH, compared with that of $J/\psi\pi$, which will strengthen TS. There is another way to understand this point. If we assume there are $Z_c(3900)$ and $Z_c(4020)$ molecular states produced in this THH loop mechanism, which corresponds to plug two propagators into the black bubble of Fig. 1(b) separately, the line shapes will be changed to some extent, as illustrated in Fig. 3. Taking into account the four types of THH loops, if we plug in $Z_c(3900)$, since it stays in the vicinity of the DD^* threshold, $\mathcal{M}^I$ will become so strong that the D_1D^* and D_2D^* cusps blur to obscurity. On the other hand, if we plug in $Z_c(4020)$ which is much closer to the D^*D^* threshold, $\mathcal{M}^{II}$ and $\mathcal{M}^{IV}$ will be strengthened, therefore the D_1D^* and D_2D^* cusps become more obvious.

The line shapes of differential cross sections also show some extraordinary phenomena. We display the results at several center of mass energy points in Fig. 3. For $J/\psi\pi$ distribution, a minicusp appeared around the DD^* threshold at $\sqrt{s} = 4.16$ GeV. With the energy increasing and being close to the D_1D threshold, TS may occur and a clear narrow cusp emerged around the DD^* threshold at $\sqrt{s} = 4.26$ GeV. With the continuous growth of the energy, the contributions of $\mathcal{M}^{II}$, $\mathcal{M}^{III}$ and $\mathcal{M}^{IV}$ become more and more significant, and the cusp around D^*D^* is emerging, but the cusp around DD^* is fading since the energy is running away from the favorable region where TS of $\mathcal{M}^I$ plays an important role. For $\psi'\pi$ and $h_c\pi$ distributions, the D^*D^* cusp has already showed up around $\sqrt{s} = 4.36$ GeV. When the energy comes to 4.415 GeV, the D^*D^* cusp becomes very obvious. It should be

mentioned these cusps are also affected by the reflection effects in the Dalitz plot.

From the above discussions, it can be concluded that the kinematics play a crucial role to produce the intriguing line shapes of total and differential cross sections. That is because TS of the THH loops has its favorable kinematic region, it is sensitive both to the masses of the internal and external states. Another important relevant factor is the phase space. These factors lead to the production of different cusps for different final states and different energy points. The $\psi'\pi\pi$ channel can be taken as a direct prediction to check this argument, since its dynamical production mechanism is the same with that of $J/\psi\pi\pi$ but the kinematics is different.

If comparing Fig. 3 with the experimental data in Refs. [10–12,15,36–40], it can be noticed that these cusps approximately fall in the corresponding vicinities of $Y(4260)$, $Y(4360)$, $Z_c(3900)/Z_c(3885)$ and $Z_c(4020)/Z_c(4025)$ in the same processes, and there are no genuine resonances introduced in this model. These cusps are generated in the dipion transitions by this special rescattering mechanism, but the open-charm channels $D_{(s)}^{(*)}D_{(s)}^{(*)}$ will not suffer from this mechanism. Therefore it will not be very surprising to observe a dip in R-value scan and open charm distributions around 4.26 and 4.36 GeV. Apart from this, there is DD^* [$Z_c(3900)$] but no D^*D^* [$Z_c(4020)$] threshold bump obtained in the $J/\psi\pi$ distribution, which is in agreement with the experimental observations [10,11]. For the $h_c\pi\pi$ channel, there is a distinct $Z_c(4020)$ signal but no significant $Z_c(3900)$ signal observed in the experiment [12]. On one hand, in our THH loop mechanism, the line shape behavior of the differential cross section is sensitive to the kinematics, and different cusps will appear for different center of mass energy $\sqrt{s}$. For instance, as illustrated in Fig. 3(f), when $\sqrt{s} = 4.26$ GeV, the DD^* cusp is much more obvious than the D^*D^* cusp. In contrast, when $\sqrt{s} = 4.415$ GeV, the D^*D^* cusp is more obvious. On the other hand, the experimental data displayed in Fig. 3(f) is a summation over data at many energy points, and the integrated luminosities and cross sections are different among these energy points [12]. Considering that in our model the relative strength of DD^* and D^*D^* cusps will change according to the center of mass energy, we qualitatively suppose that the THH loop mechanism can partly account for the experimental observation of the $h_c\pi\pi$ channel. It should be mentioned that, in Fig. 3, we incorporate some data points of the pertinent experiments, but we do not mean to fit the data considering these plots only include the contributions from THH loops.

However, just according to this simple model, the peak positions and bump structures are not precisely consistent with the current data. For instance, there is still a shifted $\psi(4160)$ bump appearing in Fig. 3(a), but this structure is not clear in experiment [36]. Another inconsistency is that DD^* cusps are stronger than D^*D^* cusps at $\sqrt{s} = 4.26$ and 4.36 GeV in Fig. 3(f) (compared with Ref. [12]), although we concluded that the strength of the cusps is sensitive to energies. To compensate for the deficiency of this simplified scenario, it seems that we need some proper interferences between the tree diagrams and THH loops. This seems to be possible, since the tree diagrams will only affect the energy region around $M_{\psi(4160)}$ according to the Breit-Wigner function Eq. (7), a proper destructive interference will possibly flatten out the bump around $\psi(4160)$. On the other hand, for $\psi'\pi\pi$ and $h_c\pi\pi$ final states, as the $\psi(4160)$ structure is already smeared, the interference may possibly make it show up again and change the D_1D cusp structure. With the center of mass energy increasing, the contribution from some other higher charmonia, such as $\psi(4415)$, will be involved. $\psi(4415)$ also stays close to the thresholds of TH, but these couplings are D wave, whose contribution will be higher order and the cusps are expected to be weakened. If we take into account S-D mixing between charmonia, $\psi(4415)$ can also couple to TH via S wave. Since its mass is closer to D_1D^* compared with D_1D, it will strengthen $\mathcal{M}^{II}$ and then strengthen the D^*D^* cusp. This may also compensate for the deficiency appearing in the $h_c\pi\pi$ channel. However, since we cannot give reliable estimations of the pertinent couplings for the moment, these are just some qualitative speculations.

There are also some theoretical uncertainties concerning our scenario. For $HH \to J/\psi(\psi')\pi$, there are two mechanisms that contribute at the same order according to the HHChPT power counting. One is the short distance process mediated by the contact interaction, as we used in our model. Another one is the t-channel process by exchanging an off shell charmed meson. For $HH \to h_c\pi$, the contribution from the second one is even at a lower order. If we take the t-channel interaction into account, it will change the triangle diagram to the box diagram. But the singular properties of the box diagram can be ascribed to the triangle diagrams, and the most important contribution still comes from the case when THH are approximately on shell. To simplify the calculation and show the intrinsic characters of the loops, i.e., TS, we will mainly discuss the triangle diagrams here. The relative strength of the rescattering amplitude will be affected by these theoretical uncertainties, but the singularity behavior of the loops is mainly in connection with the kinematics, and the line shapes will not be distorted much.

From the point of view of TS and kinematics, the model discussed here shares the similar scenario with the D_1D molecular state ansatz discussed in Refs. [34,35,41,42]. One different point is that it incorporates the D_1D, D_1D^* and D_2D^* combinations in a singe Lagrangian with the relative phase and coupling strength fixed in the heavy quark limit, which leads to most of the TH and HH cusp structures being studied simultaneously in the same channel. Another crucial point is, no matter whether the molecular state exists or not, it seems to be natural to

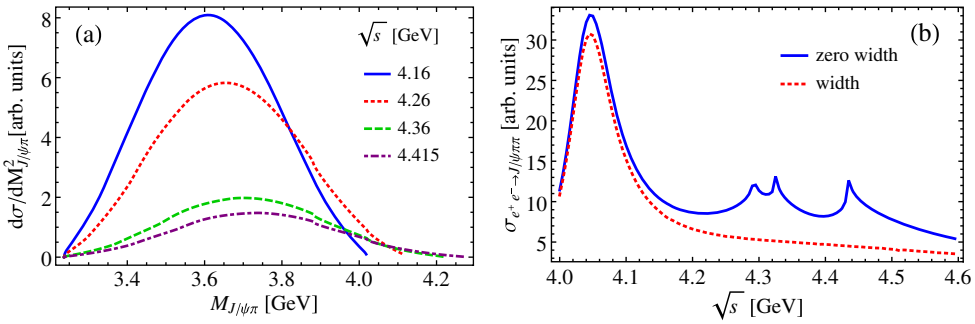

FIG. 4 (color online). (a) Differential cross section for $e^+e^- \to J/\psi\pi\pi$ via $\psi(4160)$ and intermediate HHH loops. (b) Energy dependence of the cross section for $e^+e^- \to J/\psi\pi\pi$ via $\psi(4040)$ and intermediate SHH loops, where the solid and dotted line corresponds to the result with and without taking into account the broad width influence of D_0 and D_1' respectively.

suppose the coupled-channel effects, or the vacuum polarization effects, should exist physically.

This is not the whole story concerning the rescattering processes if we only take into account the THH loops. Since experiments indicate the main decay channel of $\psi(4160)$ is HH, we should also include the contribution from HHH loops, as illustrated in Fig. 1(c). But the threshold of HH is far away from the energy region discussed here, which does not favor the kinematic conditions of TS, and the coupling between $\psi(nD)$ and HH is P wave, which will also suppress the rescattering amplitude. To make it clear, we display the differential cross section for $e^+e^- \to J/\psi\pi\pi$ in Fig. 4(a). At the center of mass energy around $\sqrt{s} = 4.16$ GeV, if the rescattering occurs via THH loops, although it is not the favorable energy point for producing singularity, there is still a visible narrow cusp appearing around the DD^* threshold. But if the rescattering occurs via HHH loops, the cusp will be nearly smeared, which is inconsistent with the result of CLEO-c [15]. This in another way supports that the coupling between $\psi(4160)$ and TH could be sizable. We also studied the rescattering processes through $\psi(nS)$ and SHH loops. As discussed in Ref. [35], since D_0 and D_1' are too broad, if taking into account their width effects, the singularities will be smoothed out and the amplitude will be lowered to some extent. We display one result in Fig. 4(b), where we have chosen $\psi(4040)$ as the intermediate S-wave charmonium [another option is $\psi(4415)$]. It can be seen that the cusps at D_0D^*, $D_1'D$, and $D_1'D^*$ are smoothed by the broad width. This is just a simple estimation, since we only change the propagators in the loops to the Breit-Winger functions, which may account for the contributions from higher order corrections. The real situation may be complicated. Although the line shape behavior of HHH and SHH loops seems to be ordinary, they can also provide some background for interference with THH loops, which is similar to the tree diagrams.

III. SUMMARY

In conclusion, we have discussed the line shape behavior of the cross sections and distributions of $e^+e^- \to J/\psi\pi\pi$, $\psi'\pi\pi$ and $h_c\pi\pi$. The coupled-channel effects, especially that induced by the couplings between the D-wave charmonia and TH charmed mesons (THH loops), are emphasized. Because these leading order S-wave couplings will respect HQSS, and another important reason is the thresholds of TH are close to that of $Y(4260)$ and $Y(4360)$. Using $\psi(4160)$ as the input $\psi(nD)$, we obtain some cusps staying at the thresholds of TH and HH, which may have some underlying connections with the XYZ states observed around these thresholds. With a few theoretical uncertainties, the line shape behavior is less model dependent, and it indicates that these cusps are sensitive to the kinematics, that is because TS of the THH loops has its favorable kinematic region. This can explain why $Z_c(3900)/Z_c(3885)$ and $Z_c(4020)/Z_c(4025)$ are observed in different processes and energy points. The $\psi'\pi\pi$ channel can be taken as a direct prediction to check this scenario.

Our paper just focuses on the dipion transitions of the charmonia, as a qualitative guess, if the coupled-channel effects with the P-wave charmed mesons involved are truly so important, maybe they can also compensate for the mass shift of charmonia sizably.

ACKNOWLEDGMENTS

The author would like to thank S. L. Zhu, Q. Zhao, F. K. Guo and G. Li for helpful discussions. This work was supported in part by the China Postdoctoral Science Foundation under Grant No. 2013M530461, the National Natural Science Foundation of China under Grants No. 11075004 and No. 11021092, and the DFG and the NSFC through funds provided to the Sino-German CRC 110 "Symmetries and the Emergence of Structure in QCD."

[1] E. Eichten, K. Gottfried, T. Kinoshita, K. D. Lane, and T.-M. Yan, Phys. Rev. D **17**, 3090 (1978); **21**, 313(E) (1980).
[2] E. J. Eichten, K. Lane, and C. Quigg, Phys. Rev. D **73**, 014014 (2006); **73**, 079903(E) (2006).
[3] M. R. Pennington and D. J. Wilson, Phys. Rev. D **76**, 077502 (2007).
[4] T. Barnes and E. S. Swanson, Phys. Rev. C **77**, 055206 (2008).
[5] B.-Q. Li, C. Meng, and K.-T. Chao, Phys. Rev. D **80**, 014012 (2009).
[6] F.-K. Guo, C. Hanhart, G. Li, Ulf-G. Meissner, and Q. Zhao, Phys. Rev. D **83**, 034013 (2011).
[7] E. van Beveren and G. Rupp, Phys. Rev. D **80**, 074001 (2009).
[8] E. van Beveren and G. Rupp, arXiv:0910.0967.
[9] Z.-Y. Zhou and Z. Xiao, arXiv:1309.1949.
[10] M. Ablikim *et al.* (BESIII Collaboration), Phys. Rev. Lett. **110**, 252001 (2013).
[11] Z. Q. Liu *et al.* (Belle Collaboration), Phys. Rev. Lett. **110**, 252002 (2013).
[12] M. Ablikim *et al.* (BESIII Collaboration), Phys. Rev. Lett. **111**, 242001 (2013).
[13] M. Ablikim *et al.* (BESIII Collaboration), Phys. Rev. Lett. **112**, 132001 (2014).
[14] M. Ablikim *et al.* (BESIII Collaboration), Phys. Rev. Lett. **112**, 022001 (2014).
[15] T. Xiao, S. Dobbs, A. Tomaradze, and K. K. Seth, Phys. Lett. B **727**, 366 (2013).
[16] X. Liu, Chin. Sci. Bull. **59**, 3815 (2014).
[17] S. L. Olsen, arXiv:1403.1254.
[18] X. Li and M. B. Voloshin, Phys. Rev. D **88**, 034012 (2013).
[19] J. Beringer *et al.* (Particle Data Group Collaboration), Phys. Rev. D **86**, 010001 (2012).
[20] M. Ablikim *et al.* (BES Collaboration), in *Proceedings of the International Workshop on Charm Physics, New York, 2007*, http://www.slac.stanford.edu/econf/C070805/; Phys. Lett. B **660**, 315 (2008).
[21] X. H. Mo, C. Z. Yuan, and P. Wang, Phys. Rev. D **82**, 077501 (2010).
[22] R. Casalbuoni, A. Deandrea, N. Di Bartolomeo, R. Gatto, F. Feruglio, and G. Nardulli, Phys. Lett. B **299**, 139 (1993).
[23] R. Casalbuoni, A. Deandrea, N. Di Bartolomeo, R. Gatto, F. Feruglio, and G. Nardulli, Phys. Rep. **281**, 145 (1997).
[24] P. Colangelo, F. De Fazio, and T. N. Pham, Phys. Rev. D **69**, 054023 (2004).
[25] T. Mehen and J. W. Powell, Phys. Rev. D **84**, 114013 (2011).
[26] A. Margaryan and R. P. Springer, Phys. Rev. D **88**, 014017 (2013).
[27] F.-K. Guo, C. Hanhart, Ulf-G. Meissner, Q. Wang, and Q. Zhao, Phys. Lett. B **725**, 127 (2013).
[28] Q. Wang, M. Cleven, F.-K. Guo, C. Hanhart, Ulf-G. Meissner, X.-G. Wu, and Q. Zhao, Phys. Rev. D **89**, 034001 (2014).
[29] L. D. Landau, Nucl. Phys. **13**, 181 (1959).
[30] R. J. Eden, P. V. Landshoff, D. I. Olive, and J. C. Polkinghorne, *The Analytic S-Matrix* (Cambridge University Press, Cambridge, England, 1966).
[31] P. V. Landshoff and S. B. Treiman, Phys. Rev. **127**, 649 (1962).
[32] P. V. Landshoff and S. B. Treiman, Nuovo Cimento **19**, 1249 (1961).
[33] J.-J. Wu, X.-H. Liu, Q. Zhao, and B.-S. Zou, Phys. Rev. Lett. **108**, 081803 (2012).
[34] Q. Wang, C. Hanhart, and Q. Zhao, Phys. Rev. Lett. **111**, 132003 (2013).
[35] X.-H. Liu and G. Li, Phys. Rev. D **88**, 014013 (2013).
[36] C. Z. Yuan *et al.* (Belle Collaboration), Phys. Rev. Lett. **99**, 182004 (2007).
[37] X. L. Wang *et al.* (Belle Collaboration), Phys. Rev. Lett. **99**, 142002 (2007).
[38] C. Z. Yuan, Chin. Phys. C **38**, 043001 (2014).
[39] B. Aubert *et al.* (*BABAR* Collaboration), arXiv:0808.1543.
[40] B. Aubert *et al.* (*BABAR* Collaboration), Phys. Rev. Lett. **98**, 212001 (2007).
[41] M. Cleven, Q. Wang, F.-K. Guo, C. Hanhart, Ulf-G. Meissner, and Q. Zhao, arXiv:1310.2190.
[42] Q. Wang, C. Hanhart, and Q. Zhao, Phys. Lett. B **725**, 106 (2013).